Science Bulletin 65 (2020) 105–112

Contents lists available at ScienceDirect

Science Bulletin

journal homepage: www.elsevier.com/locate/scib

Article

Polyaniline-TiO_2 composite photocatalysts for light-driven hexavalent chromium ions reduction

Xiaoming Deng, Yao Chen, Jieya Wen, Yun Xu, Jian Zhu *, Zhenfeng Bian *

The Education Ministry Key Laboratory of Resource Chemistry and Shanghai Key Laboratory of Rare Earth Functional Materials, Shanghai Normal University, Shanghai 200234, China

ARTICLE INFO

Article history:
Received 29 September 2019
Received in revised form 12 October 2019
Accepted 14 October 2019
Available online 21 October 2019

Keywords:
Polyaniline
Titanium dioxide
Photo-reduction
Hexavalent chromium
Trivalent chromium

ABSTRACT

In order to develop efficient photocatalysts, great efforts have been made to reduce hexavalent chromium to trivalent chromium. The photocatalytic efficiency of this reduction depends largely on the adsorption and diffusion of hexavalent chromium ions on the surface of the photocatalyst. In this paper, polyaniline-TiO_2 composite can effectively improve the photocatalytic reduction performance and stability of hexavalent chromium ion. The effect of polyaniline (PANI) thickness on Cr(VI) activity and stability of photocatalytic reduction was studied by adjusting the content of PANI on Mesoporous TiO_2 (MT) surface. Under the irradiation conditions, the reaction results showed that the reduction rate was 100%, and the maximum reaction rate reached 0.62 min^{-1} when the PANI modification was 3.0%. Moreover, the results showed that the reduction performance remained 100% after ten cycles. The main reason is that the PANI modified on the surface of TiO_2 is rich in positively charged amino group, which can efficiently adsorb the reactant Cr(VI), and make the product Cr(III) leave the reaction interface quickly, thus ensuring the performance of photocatalyst.

1. Introduction

Chromium ion is one of the common heavy metal pollutants in the environment which mainly comes from the discharge of industrial wastewater such as leather tanning, electroplating and pigments [1–4]. In water, chromium ions are mainly present in the form of Cr(VI) and Cr(III) [5]. The harm of Cr(VI) to human body is much greater than that of Cr(III) [6]. It is considered to be one of the most toxic pollutants due to its carcinogenic and mutagenic effects on organisms [7]. Therefore, removing Cr(VI) from water environment is of great significance.

At present, the main removal methods of Cr(VI) in sewage are membrane separation [8,9], ion exchange [10,11], electrodialysis [12,13] and adsorption [14–17]. Taking the adsorption method as an example, its advantage is the rapid removal of Cr(VI) in water. However, the adsorbent loses effectiveness when it reaches saturated adsorption capacity. At the same time, Cr(VI) is easily desorbed in the adsorption state, which causes secondary pollution to the environment. The key to eliminating the harm of Cr(VI) is to convert it into low-toxicity Cr(III).

Photocatalytic technology has attracted increasing attention not only for its simplicity and convenience, but also for its direct utilization of sunlight recently [18–21]. Research on photocatalytic reduction of Cr(VI) is becoming much more extensive [22,23], among which TiO_2 is the most commonly used photocatalyst [24]. In order to inhibit photogenic charge recombination and improve photocatalytic reduction performance, researchers have done a lot of work on deposition of precious metals on TiO_2 [25,26], modification of carbon materials [27], element doping [28], and coupling with narrow bandgap semiconductors [29], etc. In recent years, many studies have focused on the combination of photocatalytic reduction of Cr(VI) and degradation of organic pollutants. Gan et al. [30] used hybrid bismuth titanate $Bi_4Ti_3O_{12}$/$Bi_2Ti_2O_7$ to remove Cr(VI) and RhB in aqueous solution simultaneously. Zhang and coauthors have done a lot of research on the synergistic effect of photocatalytic reduction of Cr(VI) and degradation of methyl orange [31], as well as the photoreduction of Cr(VI) and the synergistic oxidation of phenol [32,33]. According to the previous work, we found that the desorption of Cr(III) is also very important for the photocatalytic reduction of Cr(VI) [34–36]. The desorption of Cr(III) is beneficial to prevent the surface active sites of photocatalyst from being covered and inactivated.

Polyaniline (PANI) is a good photogenerated hole transport material, which is usually combined with photocatalyst and promotes charge separation through photo-induced carrier transfer [37,38]. It is widely used in the degradation of organic pollutants by forming composite photocatalyst [39–43]. PANI not only has good acid and alkali resistance, but also has excellent stability

* Corresponding authors.
E-mail addresses: jianzhu@shnu.edu.cn (J. Zhu), bianzhenfeng@shnu.edu.cn (Z. Bian).

https://doi.org/10.1016/j.scib.2019.10.020
2095-9273/

during the photocatalytic process [44–46]. Under acidic conditions, the protonated PANI forms a positively charged amino group, which promote the absorption of Cr(VI), thereby the photocatalytic reduction process has been facilitated. Qiu et al. [47] reported that modified ethyl cellulose (EC) with PANI had much higher adsorption capacity for Cr(VI) than pure EC. Therefore, PANI has a very good prospect to be used in the photocatalytic reduction process of Cr(VI) by compounding with photocatalyst.

In this work, using Mesoporous TiO_2 (MT) as photocatalyst, PANI was modified by simple surface polymerization (Scheme 1). The catalyst exhibits remarkable enhanced photocatalytic performance and high photocatalytic stability. Firstly, PANI is rich in positively charged amino groups to effectively adsorb Cr(VI), and make Cr(III) leave the reaction interface quickly, thus promoting the photocatalytic reduction process and improving the stability of the photocatalyst. Furthermore, TiO_2 surface was modified with polyaniline, which promoted the separation of photogenic charge on TiO_2 surface and greatly improved the photocatalytic activity of the catalyst. The effect of variation of TiO_2 surface modification PANI thickness on adsorption properties of Cr(VI) and Cr(III) was described in detail. The structure of the prepared material is stable and the charge separation is strengthened. This not only provides a strategy for the preparation of high efficient photocatalyst for Cr (VI) reduction, but also opens up a new way for the wide application of photocatalysis in the field of treating heavy metal ions.

2. Experimental

MT was synthesized according to the procedures reported in Ref. [34]. Solution A was formed by dissolving 2.5 mmol of ammonium persulfate (APS) in 2 mL deionized water. 1.04 g MT was added to 10 mL deionized water for ultrasonic dispersion, and then aniline monomers of different volumes (0.01, 0.03, 0.05, 0.07, 0.10 mL) were added to form solution B. 10 mL hydrochloric acid (6 mol L^{-1}) was slowly added to solution B to form a uniform solution, which was rapidly mixed with solution A and reacted in an ice bath for 12 h. After completion of the reaction, it was washed three times with ethanol and deionized water, and then dried under vacuum at 80 °C for 24 h. The samples were named by different wt% PANI/MT. The pure PANI was successfully synthesized using the same method.

3. Results and discussions

Scanning electron microscopy (SEM) image showed that the MT sample was uniform microspheres with an average diameter of about 1 μm (Fig. 1a). The SEM and transmission electron microscopy (TEM) results showed that the surface modification of PANI had no significant effect on the morphology of MT (Fig. 1b, c and Fig. S1 (online)). As the amount of modified PANI increases, the surface of the sample is slightly rough (Fig. S1 online). TEM image

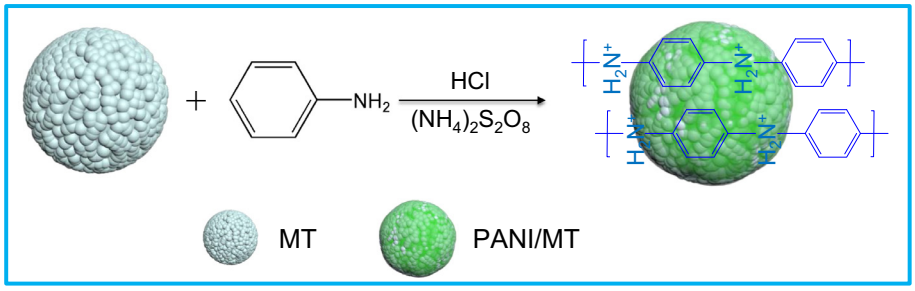

Scheme 1. (Color online) The schematic illustration for the preparation of PANI/MT sample.

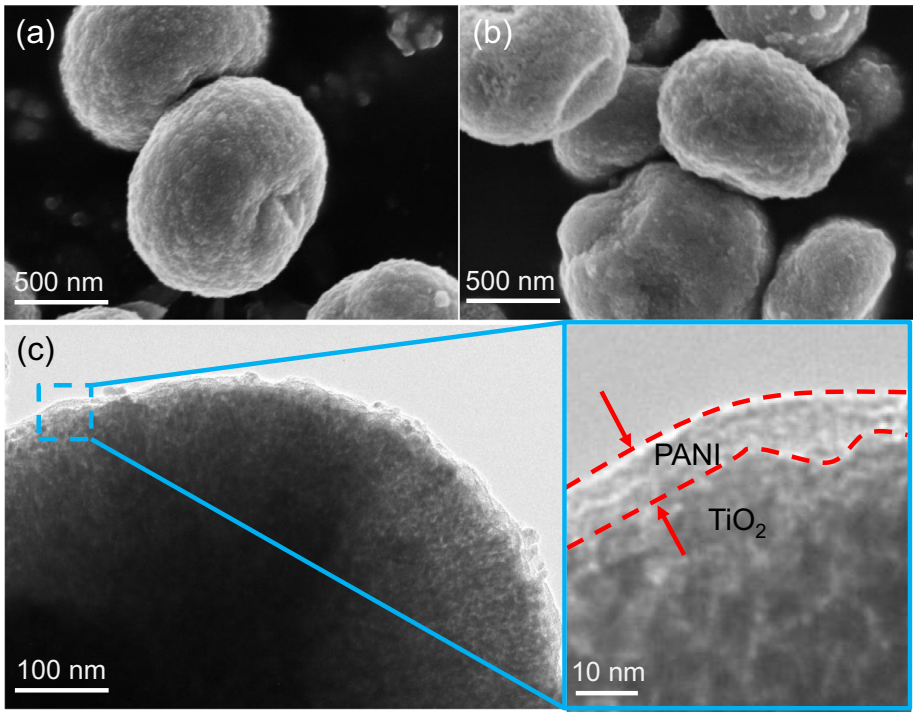

Fig. 1. (Color online) SEM images of (a) MT and (b) 3.0 wt% PANI/MT, (c) TEM image of 3.0 wt% PANI/MT.

of the 3.0 wt% PANI/MT sample showed that PANI was successfully modified on the MT surface (Fig. 1c). The TEM image (Fig. S1d online) of high-modified PANI/MT sample (20.0 wt% PANI/MT sample) showed that the surface modification layer of PANI thickens gradually with the increase of PANI modification. As seen from the FTIR spectrum (Fig. S2 online) that PANI has obvious absorption peaks around 1575, 1482, 1309, 817 and 505 cm^{-1}, which is characteristic absorption peak of PANI [48–50]. The characteristic absorption peak of PANI was clearly observed on the surface of the 3.0 wt% PANI/MT sample, indicating that PANI has been successfully modified on the surface of TiO_2.

XRD analysis showed that MT sample had typical anatase diffraction peaks (JCPDS 21-1272). MT surface modified PANI may be amorphous, so no other peaks appear in the XRD spectra of different PANI/MT samples. The results are consistent with those expressed by SEM and TEM (Fig. 2).

More importantly, some strong interactions have been formed at the interface between PANI and TiO_2, which is conducive to the separation of photogenic charges on the surface of TiO_2. As shown in Fig. 3, the high resolution N_{1s} peak of PANI was divided into two peaks at 399.4 and 400.8 eV, corresponding to —N═ and —N— groups, respectively (Fig. 3a) [51]. However, the high resolution N_{1s} peak of 3.0 wt% PANI/MT sample was distributed at 398.2, 399.7 and 401.3 eV (Fig. 3b), which can be the results of the interaction between N in PANI and Ti in TiO_2 [52]. As shown in Fig. 3c, the peak difference between $Ti_{2p3/2}$ peak at 458.4 eV and $Ti_{2p1/2}$ peak at 464.1 eV is 5.7 eV, confirming the existence of Ti^{4+} [53]. However, the $Ti_{2P3/2}$ peak of 3.0 wt% PANI/MT sample could be deconvoluted into two peaks at 457.9 and 459.3 eV (Fig. 3d). The results showed that Ti in TiO_2 and N in PANI formed strong interaction. Similarly, high resolution C_{1s} and O_{1s} spectra indicate that O in TiO_2 and C in PANI also form an interaction (Fig. S3 online). The formation of these strong interactions is conducive to the separation of photogenic charge on the surface of TiO_2 and the stable existence of PANI on the surface of TiO_2.

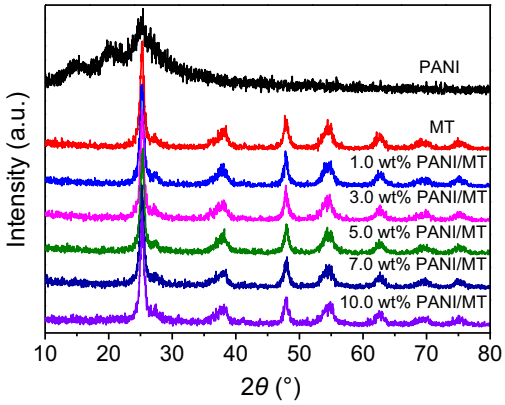

Fig. 2. (Color online) X-ray diffraction patterns of MT, different PANI/MT samples and PANI.

As shown in Fig. 4, all PANI/MT samples, including MT and PANI, were type II N_2 adsorption–desorption isotherms. According to the calculation results from N_2 desorption isotherm, compared with MT, the specific surface area (S_{BET}) of 1.0 wt% PANI/MT increased from 113 to 124 m^2/g. Similarly, the pore volume (V_p) of 1.0 wt% PANI/MT increased to 0.096 cm^3/g. This change might be due to the opening of some closed pores caused by the immersion of MT sample in hydrochloric acid solution (Fig. S4 online). Furthermore, S_{BET} and V_p of the samples decreased with the increasing

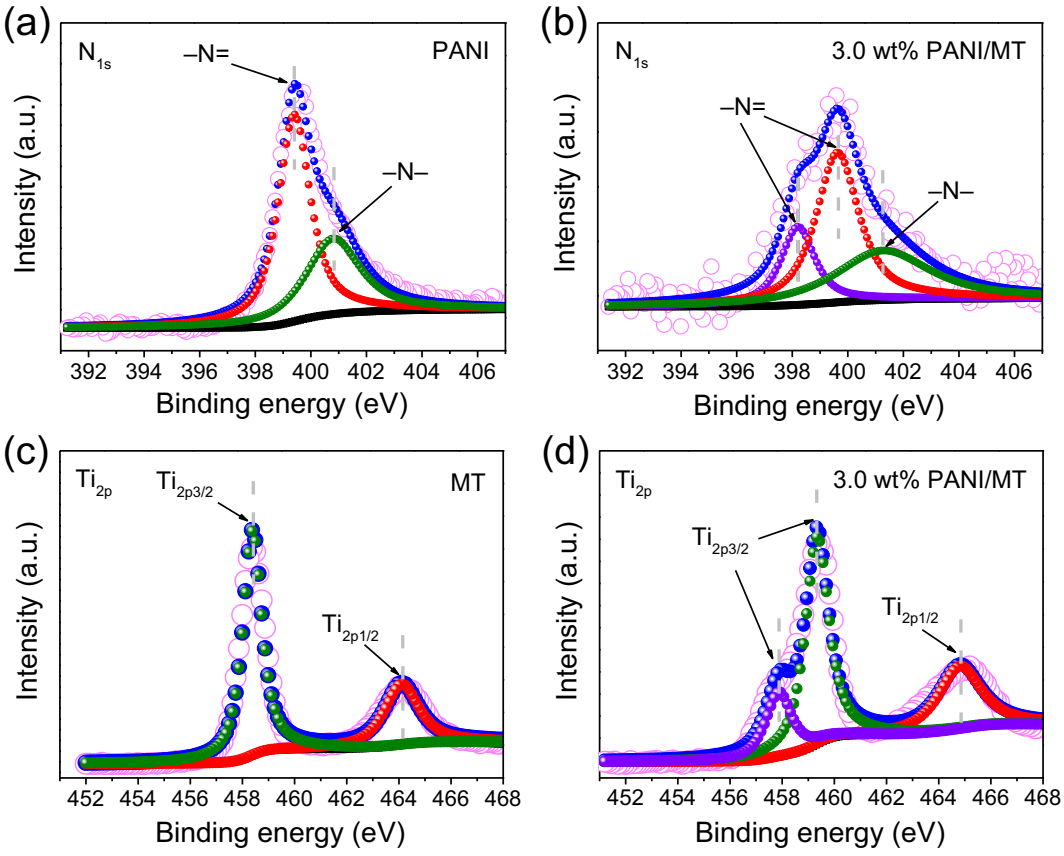

Fig. 3. (Color online) XPS spectra of PANI and 3.0 wt% PANI/MT.

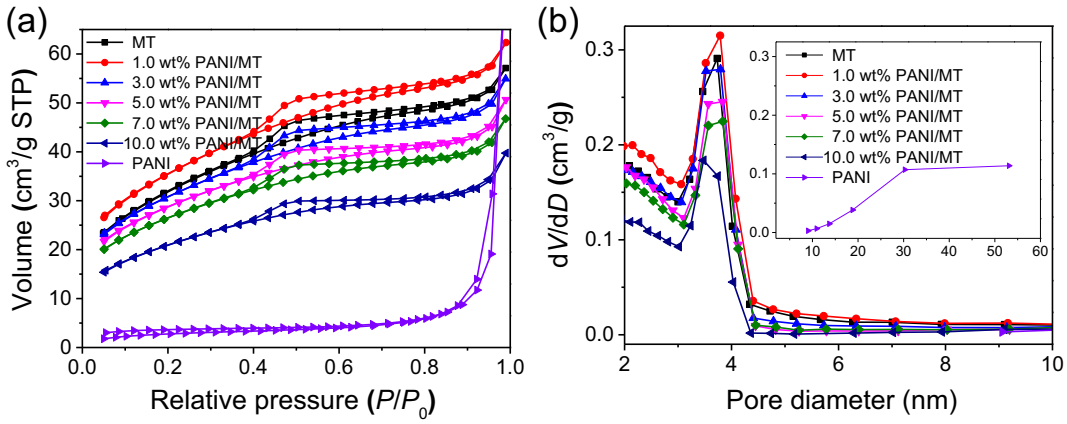

Fig. 4. (Color online) N_2 adsorption–desorption isotherms (a) and pore size distribution curves (b) of MT, different PANI/MT samples and PANI.

of PANI loading. However, the pore size of the samples did not change too much. These results indicated that PANI was highly dispersed on the surface of MT and did not completely encapsulate MT, which was beneficial to the exposure of photocatalytic reduction active site on MT surface. However, PANI modification of the MT surface resulted in a gradual clogging of the porous surface and a gradual decrease in S_{BET} and V_p, which is consistent with the results expressed by TEM and SEM.

PANI tends to protonate under acidic conditions, forming a positive amino group and having a positive surface (inset of Fig. 5). The surface zeta potential of MT modified PANI was more positive. As the PANI content increases from 0 to 5.0%, the zeta potential increases from 26 to 39 mV (Fig. 5). The potential decreased slightly with the increase of modification amount, which might be caused by PANI overload on MT surface.

In view of the negative charge of Cr(VI) and the positive charge of Cr(III), the charge on the surface of the catalyst affects the selective adsorption of chromium ions and the photocatalytic process. In order to explore the effect of surface modification on Cr(VI) and Cr(III) adsorption properties, we studied the selective adsorption of different chromium ions on different wt% PANI/MT composites (Fig. 6). The results showed that the adsorption capacity of Cr (III) decreased and that of Cr(VI) increased with the increasing modification of PANI on the surface of MT. This is mainly related to the properties of PANI which selectively adsorbs Cr(VI). This is consistent with the Zeta potential measurement results.

Under the same conditions, the photocatalytic reduction experiment of Cr(VI) was carried out. It can be seen from Fig. 7a that PANI has a very good adsorption performance for Cr(VI). Before illumination, 10 ppm Cr(VI) is adsorbed by PANI and the remaining 0.4 ppm is left. Subsequent illumination showed that there was almost no change in the residual concentration of Cr(VI), indicating that no photocatalytic reduction occurred on the surface of PANI. In the activity test of pure MT sample, after absorbing 10 ppm Cr(VI), the remaining 8 ppm Cr(VI) in the solution was obtained with an adsorption rate of 20%, reaching the adsorption equilibrium. After that, the concentration of Cr(VI) continued to decrease and photocatalytic reduction of Cr(VI) occurred. As the PANI load on the MT surface increases, the adsorption capacity of Cr(VI) on the surface of the sample in the light-off stage gradually increases. After 6 min of illumination, the Cr(VI) in the solution could hardly be detected. Kinetic studies show that Cr(V) reduction conforms to the quasi-first-order reaction expression of the simplified Langmuir-Hinshelwood model (Fig. 7b). According to the calculated rate constant, the reaction rate of 3.0 wt% PANI/MT sample is the highest, which is twice that of MT sample. The improvement of photocatalytic performance may be due to the enrichment of Cr (VI) on the surface of the catalyst, which promotes the degradation rate to a certain extent; on the other hand, the modification of PANI on the surface of the catalyst is conducive to the separation of photogenerated charges.

Modification of MT with PANI is beneficial to the separation of photogenerated charges and the formation of heterojunction between them, reducing photoelectron-hole recombination (Fig. 8a) [39]. The results of photocurrent measurements show that PANI modification can improve the photocurrent response of MT

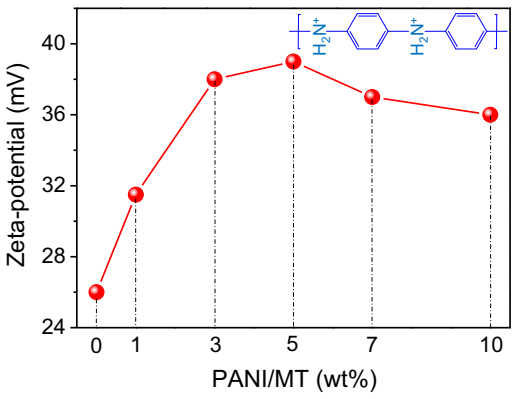

Fig. 5. (Color online) Zeta potentials of MT and different PANI/MT samples (pH 3.0). The inset is the protonation of PANI under acidic conditions.

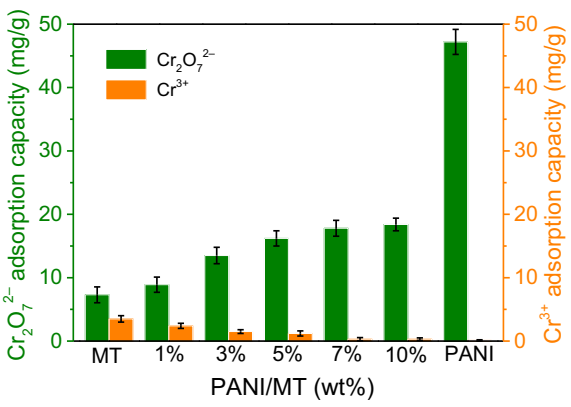

Fig. 6. (Color online) Adsorption capacities for Cr(VI)/Cr(III) on different PANI/MT samples (pH 3.0).

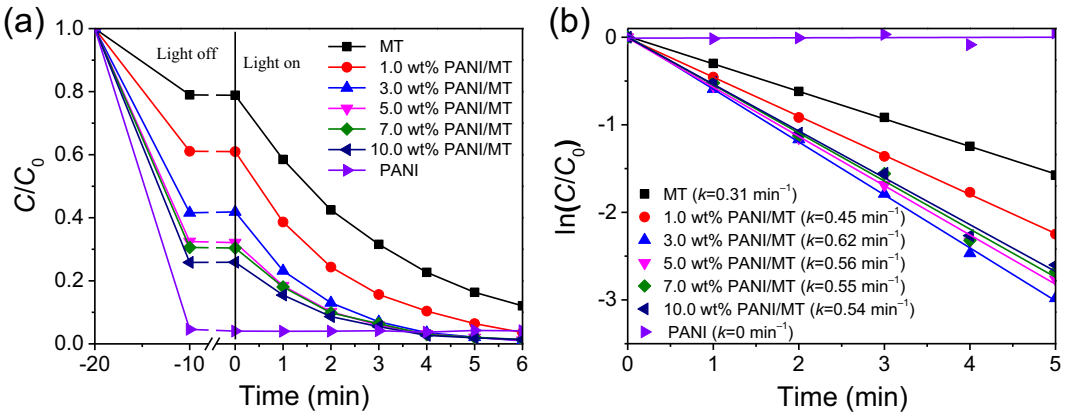

Fig. 7. Liquid-phase photocatalytic Cr(VI) anion reduction (a) and kinetic linear fitting curves (b) on different samples (pH 3.0); $\ln(C_0/C_t) = kt$, where C_t is the concentration of organics at time t, and k is the apparent first-order rate constant.

samples and the separation of photogenerated charges (Fig. 8b). However, high PANI modification is not conducive to the surface photocurrent. The possible reason is that the ultraviolet light is absorbed by PANI as the amount of modified PANI increases on the MT surface (Fig. 8c). The same results were also shown in the surface photovoltage test (Fig. 8d). Therefore, the reaction rate decreases slightly with the increasing amount of PANI modification.

The photocatalytic stability and durability of the MT was improved by surface modification of PANI. As shown in Fig. 9, the removal rate of Cr(VI) in the 3.0 wt% PANI/MT sample was still 100% after 10 times of photocatalytic reduction of Cr(VI) reactions. The removal yield of MT was 26% (almost inactivated) after 10 times reaction. To investigate the cause of photocatalytic deactivation, we tested MT samples after 10 cycles using XPS. As shown in Fig. S5 (online), a large amount of Cr(III) was deposited on the surface of MT samples after 10 cycles of photocatalytic reduction of Cr (VI). This indicates that the inactivation of MT samples is caused by the large amount of photocatalytic sites covered by surface deposited Cr(III). The durability and stability of 3.0 wt% PANI/MT composites are high because of the existence of positively charged amino groups on the surface of the composites, which is conducive to the rapid separation of Cr(III) cations in the photocatalytic reduction process. To further explore the influence of the thickness of PANI modified on the surface of MT on photocatalyst stability, we conducted the same test on 10.0 wt% PANI/MT sample (Fig. 9). After 10 times of reaction, the removal rate of Cr(VI) in 10.0 wt% PANI/MT sample was 61%, and the stability was decreased. This may be due to the longer migration path of Cr

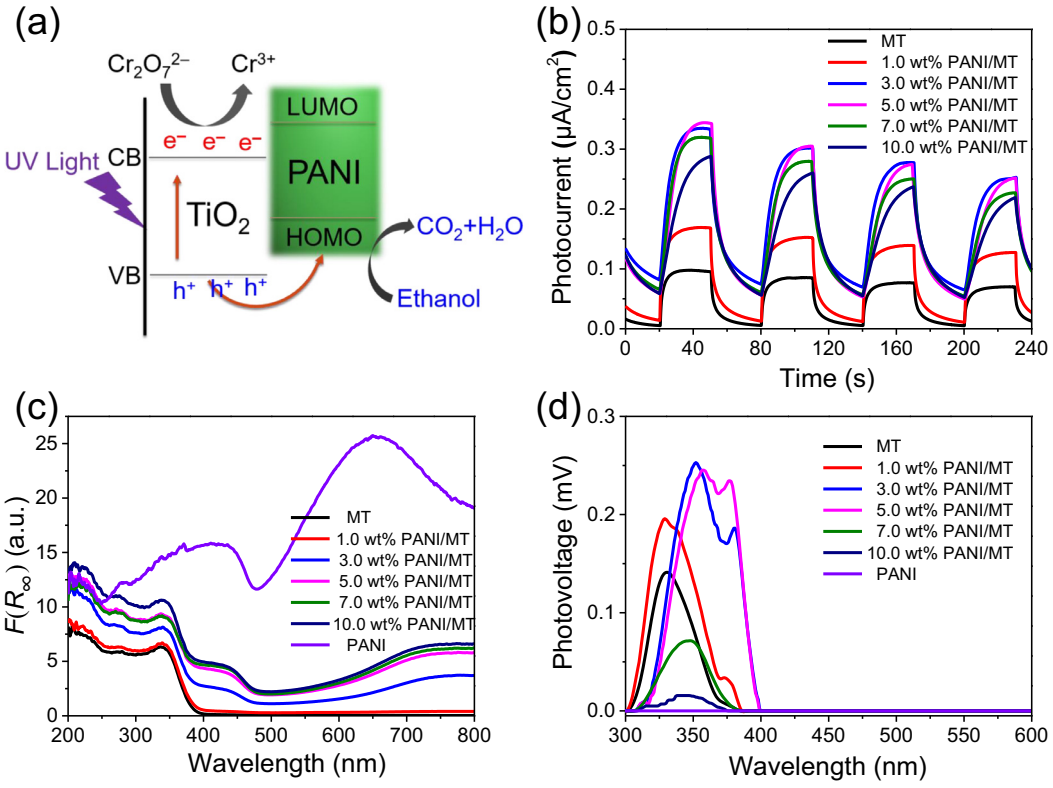

Fig. 8. The photoelectric performance: (a) mechanism scheme of UV photocatalysis process, (b) photocurrent responses of different PANI/MT samples under UV light irradiation, (c) UV–Vis diffuse reflectance spectra of different PANI/MT samples and (d) surface photovoltage responses of different PANI/MT samples.

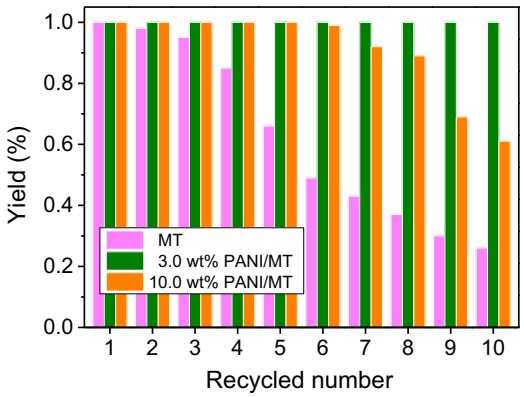

Fig. 9. Recycling tests of the MT, 3.0 wt% PANI/MT sample and 10.0 wt% PANI/MT sample (pH 3.0).

(III) from MT surface to solution caused by the increase of PANI thickness, and Cr(III) deposition on catalyst surface gradually increased.

Meanwhile, 3.0 wt% PANI/MT sample was used to carry out photocatalytic reduction under different concentrations of Cr(VI) (Fig. 10). The results show that the higher the concentration of the Cr(V) solution, the slower the photocatalytic reaction rate. When the Cr(VI) solution concentration is 50 ppm, the photocatalytic reduction rate is reduced to 0.02 min^{-1}, which is only 1/31 of the Cr(VI) solution concentration of 10 ppm. When the concentration of the Cr(VI) solution is too high, the reactant product Cr(III) cannot be quickly separated from the surface of the catalyst to deposit on the surface of the catalyst, causing the photoreduction active site to be covered, and the photocatalytic activity is thus lowered. The result is consistent with that shown in Fig. 9, indicating that rapid separation of Cr(III) from the catalyst surface is an important way to improve the activity and stability of photocatalytic reduction of hexavalent chromium.

Based on the above results, we further proposed the photocatalytic reduction mechanism of Cr(VI) on PANI/MT sample surface (Fig. 11). Under acidic conditions, the positively charged amino groups on PANI were easy to adsorb the negatively charged Cr (VI) and repel the positively charged Cr(III). PANI can greatly improve the separation efficiency of photogenerated charge due to its high stability and good photogenerated hole transport materials (Fig. 8a). The rapid adsorption of Cr(VI) contributes to the photocatalytic reduction of Cr(VI) to Cr(III). Rapid desorption of Cr(III) on PANI/MT catalysts improves the activity and durability of

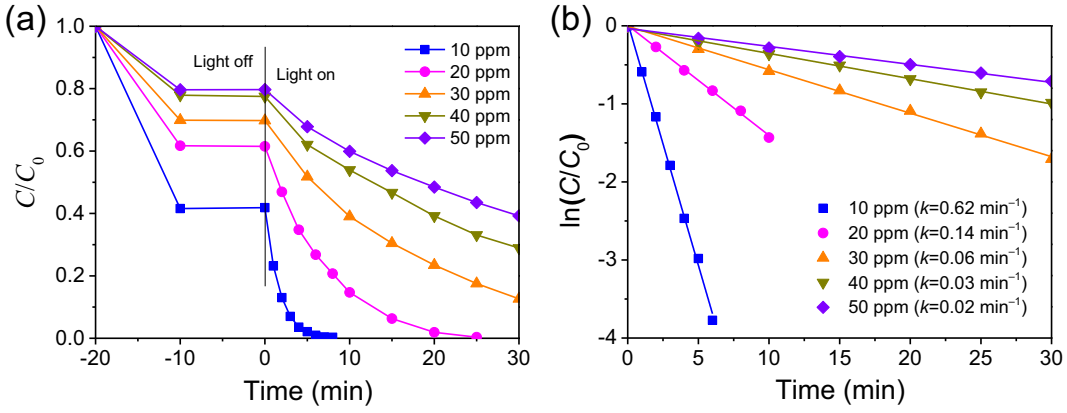

Fig. 10. Liquid-phase photocatalytic reduction of various concentrations of Cr(VI) (a) and kinetic linear fitting curves (b) on 3.0 wt% PANI/MT sample.

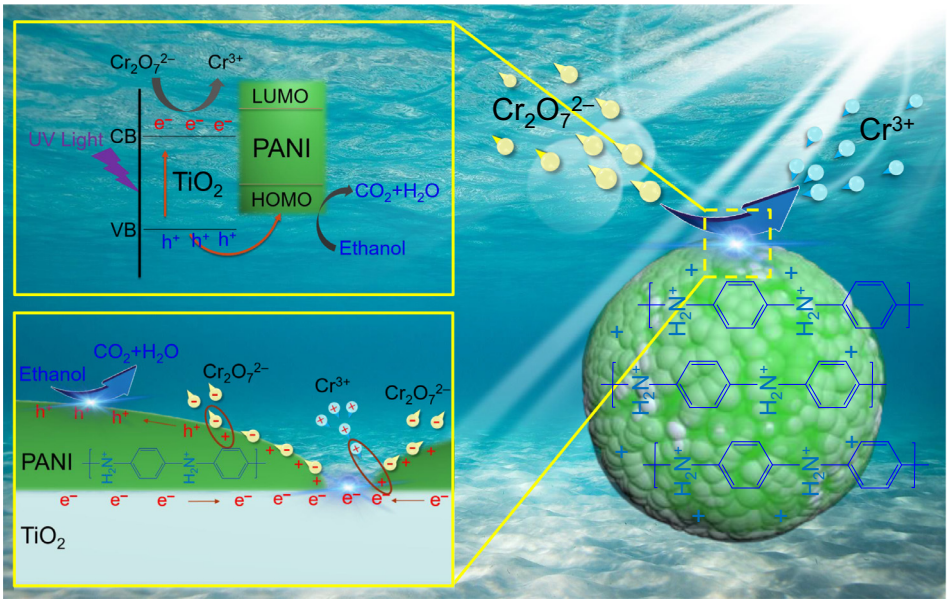

Fig. 11. A proposed adsorption-photoreduction-desorption mechanisms of photocatalytic reduction of Cr(VI) in the presence of PANI/MT composite.

photocatalytic reduction from Cr(VI) to Cr(III) and realizes the efficient regeneration of photocatalysts.

4. Conclusion

In summary, the surface of MT was modified with PANI, which is the active site for promoting photogenerated charge separation and Cr(VI) adsorption. PANI/MT with a mass fraction of 3.0 wt% was almost twice as active as MT in the photocatalytic reduction of Cr(VI). After 10 cycles of the reaction, 3.0 wt% PANI/MT still maintained 100% removal of Cr(VI), while MT was inactivated. The positively charged amino group on the protonated polyaniline facilitates the adsorption of the negatively charged hexavalent chromium anion ($Cr_2O_7^{2-}$) and exclusion of positively charged chromium trivalent cation (Cr^{3+}), thereby promoting the process of photoreduction of Cr(VI) to Cr(III). Moreover, the surface-modified polyaniline is beneficial for promoting charge separation on the surface of MT and enhancing photocatalytic activity. This work provides a new idea for sustainable treatment of Cr(VI) in water environment.

Conflict of interest

The authors declare that they have no conflict of interest.

Acknowledgments

This work was supported by the National Natural Science Foundation of China (21876114, 21761142011, and 51572174), Shanghai Government (19160712900), International Joint Laboratory on Resource Chemistry (IJLRC), and Ministry of Education of China (PCSIRT_IRT_16R49). And this work was also supported by The Program for Professor of Special Appointment (Eastern Scholar) at Shanghai Institutions of Higher Learning and Shuguang Research Program of Shanghai Education Committee.

Author contributions

Xiaoming Deng charted the figures and tables. Yao Chen, Jieya Wen and Yun Xu collected and analyzed the literatures. Zhenfeng Bian and Xiaoming Deng wrote the original draft. Jian Zhu and Zhenfeng Bian reviewed and edited the draft.

Appendix A. Supplementary materials

Supplementary materials to this article can be found online at https://doi.org/10.1016/j.scib.2019.10.020.

References

[1] Blowes D. Tracking hexavalent Cr in groundwater. Science 2002;295:2024–5.
[2] Costa M. Potential hazards of hexavalent chromate in our drinking water. Toxicol Appl Pharmacol 2003;188:1–5.
[3] Gu H, Rapole SB, Huang Y, et al. Synergistic interactions between multi-walled carbon nanotubes and toxic hexavalent chromium. J Mater Chem A 2013;1:2011–21.
[4] Vaiopoulou E, Gikas P. Effects of chromium on activated sludge and on the performance of wastewater treatment plants: a review. Water Res 2012;46:549–70.
[5] Lin C, Wang S, Huang P, et al. Chromate reduction by zero-valent Al metal as catalyzed by polyoxometalate. Water Res 2009;43:5015–22.
[6] Guo L, Xiao Y, Wang Y. Hexavalent chromium-induced alteration of proteomic landscape in human skin fibroblast cells. J Proteome Res 2013;12:3511–8.
[7] Linos A, Petralias A, Christophi CA, et al. Oral ingestion of hexavalent chromium through drinking water and cancer mortality in an industrial area of Greece-An ecological study. Environ Health 2011;10:50.
[8] Chen JH, Le T, Hsu KC. Application of PolyHIPE membrane with tricaprylmethylammonium chloride for Cr(VI) ion separation: parameters and mechanism of transport relating to the pore structure. Membranes 2018;8:11.
[9] Liu J, Zhang W, Ren Z, et al. The separation and concentration of Cr(VI) from acidic dilute solution using hollow fiber renewal liquid membrane. Ind Eng Chem Res 2009;48:4500–6.
[10] Edebali S, Pehlivan E. Evaluation of Amberlite IRA96 and Dowex 1×8 ion-exchange resins for the removal of Cr(VI) from aqueous solution. Chem Eng J 2010;161:161–6.
[11] Xing Y, Chen X, Wang D. Electrically regenerated ion exchange for removal and recovery of Cr(VI) from wastewater. Environ Sci Technol 2007;41:1439–43.
[12] Barrera CE, Lugo V, Bilyeu B. A review of chemical, electrochemical and biological methods for aqueous Cr(VI) reduction. J Hazard Mater 2012;223–224:1–12.
[13] Peng C, Meng H, Song S, et al. Elimination of Cr(VI) from electroplating wastewater by electrodialysis following chemical precipitation. Sep Sci Technol 2004;39:1501–17.
[14] Bhattacharya AK, Naiya TK, Mandal SN, et al. Adsorption, kinetics and equilibrium studies on removal of Cr(VI) from aqueous solutions using different low-cost adsorbents. Chem Eng J 2008;137:529–41.
[15] Selvi K, Pattabhi S, Kadirvelu K. Removal of Cr(VI) from aqueous solution by adsorption onto activated carbon. Bioresour Technol 2001;80:87–9.
[16] Guo Y, Qi J, Yang S. Adsorption of Cr(VI) on micro- and mesoporous rice husk-based active carbon. Mater Chem Phys 2003;78:132–7.
[17] Kobya M. Removal of Cr(VI) from aqueous solutions by adsorption onto hazelnut shell activated carbon: kinetic and equilibrium studies. Bioresource Technol 2004;91:317–21.
[18] Wang L, Jin P, Duan S, et al. In-situ incorporation of Copper(II) porphyrin functionalized zirconium MOF and TiO_2 for efficient photocatalytic CO_2 reduction. Sci Bull 2019;64:926–33.
[19] Gao X, An L, Qu D, et al. Enhanced photocatalytic N_2 fixation by promoting N_2 adsorption with a co-catalyst. Sci Bull 2019;64:918–25.
[20] Feng Y, Li H, Ling L, et al. Enhanced photocatalytic degradation performance by fluid-induced piezoelectric field. Environ Sci Technol 2018;52:7842–8.
[21] Xu M, Chen Y, Qin J, et al. Unveiling the role of defects on oxygen activation and photodegradation of organic pollutants. Environ Sci Technol 2018;52:13879–86.
[22] Luan S, Qu D, An L, et al. Enhancing photocatalytic performance by constructing ultrafine TiO_2 nanorods/g-C_3N_4 nanosheets heterojunction for water treatment. Sci Bull 2018;63:683–90.
[23] Yue D, Qian X, Zhao Y. Photocatalytic remediation of ionic pollutant. Sci Bull 2015;60:1791–806.
[24] Testa JJ, Grela MA, Litter MI. Heterogeneous photocatalytic reduction of chromium(VI) over TiO_2 particles in the presence of oxalate: involvement of Cr (V) species. Environ Sci Technol 2004;38:1589–94.
[25] Choi Y, Koo MS, Bokare AD, et al. Sequential process combination of photocatalytic oxidation and dark reduction for the removal of organic pollutants and Cr(VI) using Ag/TiO_2. Environ Sci Technol 2017;51:3973–81.
[26] Pan X, Xu YJ. Defect-Mediated growth of Noble-Metal (Ag, Pt, and Pd) nanoparticles on TiO_2 with oxygen vacancies for photocatalytic redox reactions under visible light. J Phys Chem C 2013;117:17996–8005.
[27] Tan X, Fang M, Wang X. Preparation of TiO_2/multiwalled carbon nanotube composites and their applications in photocatalytic reduction of Cr(VI) study. J Nanosci Nanotechnol 2008;8:5624.
[28] Zhang Y, Yang M, Zhang G, et al. HNO_3-involved one-step low temperature solvothermal synthesis of N-doped TiO_2 nanocrystals for efficient photocatalytic reduction of Cr(VI) in water. Appl Catal B 2013;142–143:249–58.
[29] Zhang Y, Li J, Xu H. One-step in-situ solvothermal synthesis of SnS_2/TiO_2 nanocomposites with high performance in visible light-driven photocatalytic reduction of aqueous Cr(VI). Appl Catal B 2012;123–124:18–26.
[30] Gan H, Liu J, Zhang H, et al. Enhanced photocatalytic removal of hexavalent chromium and organic dye from aqueous solution by hybrid bismuth titanate $Bi_4Ti_3O_{12}$/$Bi_2Ti_2O_7$. Res Chem Intermediat 2018;44:2123–38.
[31] Chen C, Xun L, Zhang P, et al. Z-scheme structure SnS_2–Au–CdS with excellent photocatalytic performance for simultaneous removal of Cr(VI) and methyl orange. Res Chem Intermediat 2019;45:3513–24.
[32] Liu J, Fang W, Wang Y, et al. Gold-loaded graphene oxide/PDPB composites for the synchronous removal of Cr(VI) and phenol. Chin J Catal 2018;39:8–15.
[33] Liu F, Yu J, Tu G, et al. Carbon nitride coupled Ti-SBA15 catalyst for visible-light-driven photocatalytic reduction of Cr(VI) and the synergistic oxidation of phenol. Appl Catal B 2017;201:1–11.
[34] Zhang Y, Xu M, Li H, et al. The enhanced photoreduction of Cr(VI) to Cr(III) using carbon dots coupled TiO_2 mesocrystals. Appl Catal B 2018;226:213–9.
[35] Li Y, Bian Y, Qin H, et al. Photocatalytic reduction behavior of hexavalent chromium on hydroxyl modified titanium dioxide. Appl Catal B 2017;206:293–9.
[36] Qin H, Bian Y, Zhang Y, et al. Effect of Ti(III) surface defects on the process of photocatalytic reduction of hexavalent chromium. Chin J Chem 2017;35:203–8.
[37] Xiong S, Phua SL, Dunn BS, et al. Covalently bonded polyaniline–TiO_2 hybrids: a facile approach to highly stable anodic electrochromic materials with low oxidation potentials. Chem Mater 2009;22:255–60.

[38] Chen L, Yang S. Interface engineering of TiO_2@PANI nanostructures for efficient visible-light activation. Bull Mater Sci 2018;41:146.
[39] Zhang H, Zong R, Zhao J. Dramatic visible photocatalytic degradation performances due to synergetic effect of TiO_2 with PANI. Environ Sci Technol 2008;42:3803–7.
[40] Cui W, He J, Wang H, et al. Polyaniline hybridization promotes photo-electrocatalytic removal of organic contaminants over 3D network structure of rGH-PANI/TiO_2 hydrogel. Appl Catal B 2018;232:232–45.
[41] Chen F, An W, Li Y, et al. Fabricating 3D porous PANI/TiO_2-graphene hydrogel for the enhanced UV-light photocatalytic degradation of BPA. Appl Surf Sci 2018;427:123–32.
[42] Gilja V, Vrban I, Mandic V, et al. Preparation of a PANI/ZnO composite for efficient photocatalytic degradation of acid blue. Polymers 2018;10:940.
[43] Hung CH, Yuan C, Li HW. Photodegradation of diethyl phthalate with PANi/CNT/TiO_2 immobilized on glass plate irradiated with visible light and simulated sunlight-effect of synthesized method and pH. J Hazard Mater 2017;322:243–53.
[44] Melitas N, Chuffe-Moscoso O, Farrell J. Kinetics of soluble chromium removal from contaminated water by zerovalent iron media: corrosion inhibition and passive oxide effects. Environ Sci Technol 2001;35:3948–53.
[45] Olad A, Nabavi R. Application of polyaniline for the reduction of toxic Cr(VI) in water. J Hazard Mater 2007;147:845–51.
[46] Sun XF, Ma Y, Liu XW, et al. Sorption and detoxification of chromium(VI) by aerobic granules functionalized with polyethylenimine. Water Res 2010;44:2517–24.
[47] Qiu B, Xu C, Sun D, et al. Polyaniline coated ethyl cellulose with improved hexavalent chromium removal. ACS Sustain Chem Eng 2014;2:2070–80.
[48] Stejskal J, Sapurina I, Trchová M, et al. Oxidation of aniline: polyaniline granules, nanotubes, and oligoaniline microspheres. Macromolecules 2012;41:3530–6.
[49] Chen D, Zhang F, Wang W, et al. Synergistic effect of PANI and $NiFe_2O_4$ for photocatalytic hydrogen evolution under visible light. Int J Hydrog Energy 2018;43:2121–9.
[50] Tian Y, Li W, Zhao C, et al. Fabrication of hollow mesoporous SiO_2-BiOCl@PANI@Pd photocatalysts to improve the photocatalytic performance under visible light. Appl Catal B 2017;213:136–46.
[51] Liu F, Huang L, Wen T, et al. Large-area network of polyaniline nanowires supported platinum nanocatalysts for methanol oxidation. Synthetic Met 2007;157:651–8.
[52] Lv H, Wang Y, Pan L, et al. Patterned polyaniline encapsulated in titania nanotubes for electrochromism. Phys Chem Chem Phys 2018;20:5818–26.
[53] Zeng L, Song W, Li M, et al. Catalytic oxidation of for-maldehyde on surface of H-TiO_2/H-C-TiO_2 without light illumination at room temperature. Appl Catal B 2014;147:490–8.

Xiaoming Deng is a master degree candidate of industrial catalysis in Shanghai Normal University. His main research is the preparation of new titanium dioxide materials and photocatalytic treatment of hexavalent chromium ions in sewage.

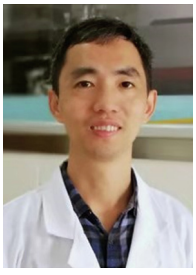

Jian Zhu received his Ph.D. degree from Fudan University in 2007. He is currently a full professor in the Department of Chemistry, Shanghai Normal University. He is an active young scientist in photocatalysis field. His main research interest is in the area of TiO_2 based semiconductors and their applications in photocatalysis and energy storage.

Zhenfeng Bian received his Ph.D. degree in Environmental Chemistry from the Shanghai Normal University in 2010. He has been a JSPS Postdoctoral Fellow in the laboratory of Professor Tetsuro Majima during 2010–2013. He became a Professor in the Department of Chemistry at Shanghai Normal University in 2013. His research interests are focused on the design and synthesis of TiO_2-based nanomaterials for environmental and energy photocatalysis.